# Designing of Sparse 2D Arrays for Lamb Wave Imaging Using Coarray Concept

Łukasz Ambroziński[†], Tadeusz Stepinski[*] and Tadeusz Uhl[*]

[*]*AGH University of Science and technology, al. Mickiewicza 30, 30-059 Krakow, Poland*
[†]*ambrozin@agh.edu.pl*

**Abstract.** 2D ultrasonic arrays have considerable application potential in Lamb wave based SHM systems, since they enable equivocal damage imaging and even in some cases wave-mode selection. Recently, it has been shown that the 2D arrays can be used in SHM applications in a synthetic focusing (SF) mode, which is much more effective than the classical phase array mode commonly used in NDT. The SF mode assumes a single element excitation of subsequent transmitters and off-line processing the acquired data. In the simplest implementation of the technique, only single multiplexed input and output channels are required, which results in significant hardware simplification. Application of the SF mode for 2D arrays creates additional degrees of freedom during the design of the array topology, which complicates the array design process, however, it enables sparse array designs with performance similar to that of the fully populated dense arrays. In this paper we present the coarray concept to facilitate synthesis process of an array's aperture used in the multistatic synthetic focusing approach in Lamb waves-based imaging systems. In the coherent imaging, performed in the transmit/receive mode, the sum coarray is a morphological convolution of the transmit/receive sub-arrays. It can be calculated as the set of sums of the individual sub-arrays' elements locations. The coarray framework will be presented here using a an example of a star-shaped array. The approach will be discussed in terms of beampatterns of the resulting imaging systems. Both simulated and experimental results will be included.

## INTRODUCTION

Radar [1], ultrasonic imaging in medical [2], nondestructive testing (NDT) [3] and structural health monitoring (SHM) [4] are examples of applications in which 2D arrays of transducers are used. Significant number of elements, used in the 2D topologies results normally in a high hardware complexity. When an array operates in an active phased array mode in real time its elements are used to excite waves that are steered to and focused at the desired point. This approach normally requires separate transmission and reception channels for each element in the array. Moreover, the transmission has to be repeated for numerous points to cover the whole region of interest (ROI) [4].

Another solution is synthetic focusing (SF) approach where focusing is performed post-acquisition. In the SF technique single elements of transmit aperture are sequently fired, whereas all elements of the receiving aperture are used to sense the scattered waves. At most, *full matrix* of transmit-receive data that consist of $N^2$ time-traces can be obtained using an array consisting of $N$ elements [5].

Collection of the full data matrix may take a significant time period and its further processing demands a considerable computation effort. Therefore, sparse arrays that use only a reduced number of elements for transmission/reception have been introduced. These arrays can benefit both in medical and industrial NDT applications, mainly due to shortened acquisition time, however, hardware simplification and reduced computation demands are important advantages of sparse arrays also in SHM applications.

In the design process of sparse arrays the transmitting and receiving apertures and their apodization are formed in the way that does not reduce their spatial resolution comparing to fully populated array [6]. The signal loss resulting form the reduced number of transmitting elements can in many cases be compensated by increasing energy delivered to a single transmitter [7].

When two apertures contribute to coherent imaging, their far-field effective aperture can be evaluated as a spatial convolution of these apertures. It appears that this operation can be easily interpreted using coarray concept [8]. This approach enables thorough investigation of the geometrical extent and apodization of the resulting aperture that is particularity useful for the synthesis of 2D apertures.

In this paper the coarray concept will be used to describe the 2D aperture synthesis for Lamb waves imaging. First, the theoretical background will be introduced and the framework will be explained using a sparse linear array.

*41st Annual Review of Progress in Quantitative Nondestructive Evaluation*
AIP Conf. Proc. 1650, 192-201 (2015); doi: 10.1063/1.4914610

Application of the coarray concept for a uniform linear array is straightforward, i.e. the shape, redundancy of the resulting coarray is easy to predict. Some simple 2D shapes have coarrays that can be also easily predicted. For instance a cross-shaped array consisting of a linear transmitting and linear receiving array lead to square coarray [9]. However, the advantages of the coarray concept are more apparent when it is applied for a more complex 2D shape. Therefore, here, a 2D star-shaped transmit-receive array will be discussed and analyzed next using numerical simulations and experimental data.

# THEORY

## Effective Aperture and Coarray

In general, any combination of sparse transmitting/receiving apertures can be used in each measurement cycle to provide data for imaging algorithms that can take advantage of numerous snapshots acquired for a range of different emitters'/sensors' configurations. If the beamforming instrumentation is capable of switching between the transmission and reception of the elements the full matrix of transmit-receive data can be captured. Although, the full matrix offers the largest amount of information, which can be gathered from an array at a fixed position, its collection can be time-consuming and hence impractical in many applications [6, 7].

Sparsely populated apertures can be used as a compromise between image quality and acquisition time expressed in the amount of images per time unit by means of the SA approach. The main idea is to effectively use transducers grouped into transmitting and receiving sub-arrays. The elements of a transmitting aperture can be fired in the same transmission cycle to obtain a steered wave front. Alternatively, individual transmitters can be excited separately while multiple responses are acquired by the elements of the receiving aperture. The snapshots of the acquired back-scattered signals can be then used for synthetic focusing during post-processing. When two sub-arrays contribute to imaging, the resulting radiation pattern of the whole active array can be evaluated using the effective aperture concept.

The *effective aperture* of an array is defined as en equivalent receive aperture that would produce an identical two-way radiation pattern if a point source was used for the transmission [10].

Assuming far-field imaging the effective aperture can be calculated as a convolution of the transmission and reception apertures [6, 7]. Let the the aperture functions $w_T(T)$ and $w_R(R)$ represent the transmission and reception apertures, respectively, then the effective aperture $w_{TR}(C_s)$ is

$$w_{TR}(C_s) = w_T(T) * w_R(R), \tag{1}$$

where $T$, $R$ and $C_s$ are sets of vectors denoting location of elements in the transmitting, receiving and effective apertures, respectively. The coordinates of the $C_s$ and hence geometrical properties of the resulting effective aperture can be expressed as a *sum coarray* (SCA), defined as the set of vector sums of formed from the location vectors of all discrete points in the apertures. In the presented coherent imaging case the SCA of a pair of apertures can be calculated as

$$C_s = \left\{ \vec{s} \,|\vec{s} = \vec{s}_i + \vec{s}_j, \quad for\ \vec{s}_i \in T\ and\ \vec{s}_j \in R \right\}. \tag{2}$$

In many cases numerous independent transmission and reception cycles are used to form a single image. The total effective aperture in SA is then the sum of all effective apertures resulting from these firings

$$w_{TR}^{SA}(C_s) = \sum_{n=1}^{N_f} w_{T_n}(T_n) * w_{R_n}(R_n), \tag{3}$$

where $N_f$ is the number of independent firings, $w_{T_n}$ and $w_{R_n}$ are weighting functions used at firing $n$ for apodization of the apertures consisting of elements from the sets $T_n$ and $R_n$, respectively. Note that the collection $C_s$ in eq. (2) is supplemented with the sum of vectors which were not already there. If the array consisting of $M$ elements is nonuniformly sampled, and there are no repeated vector sums, the maximum number of distinct elements in the coarray is $M(M+1)/2$ [8].

Using the coarray concept the effective aperture can be considered as an equivalent receiving aperture consisting of virtual receiving elements localized at locations described by the set of vectors of the sum coarray $C_s$. The signal that would be measured by a virtual element at aperture resulting from a transmission from a single element at the origin of the aperture plane is called the *coarray observation function* [8].

The signals corresponding to these elements contribute to imaging with defined weights. In the case of *nonredundant* coarray, that was formed by distinct vectors sums, the weight of $m$th coarray element can be calculated simply as a product of weights of the transmitter and receiver that were used to create the $m$th element

$$w_{TR}(\vec{s}_m) = w_T(\vec{s}_i) \cdot w_R(\vec{s}_j), \tag{4}$$

where $\vec{s}_m = \vec{s}_i + \vec{s}_j$. Therefore, the resulting value is one if a uniform weighting was assumed for the transmitting and receiving apertures.

In general case, however, more than one transmitter/receiver pair can lead to the same $m$th coarray element. In this case the coarray is *redundant* which can be interpreted as $N_r$ repetitions of the acquisition cycles performed by $m$th virtual element, where $N_r$ is the number of transmitter/receiver pairs with the same location vectors sums, or in other words, the same coarray observation function is used several times for imaging. Then the weight of $m$th coarray element can be found as

$$w_{TR}(\vec{s}_m) = \sum_{n=1}^{N_r} w_{Tn}(\vec{s}_{in}) \cdot w_{Rn}(\vec{s}_{jn}), \tag{5}$$

for all $\vec{s}_{in}$ and $\vec{s}_{jn}$ satisfying $\vec{s}_m = \vec{s}_{in} + \vec{s}_{jn}$. Consequently, in this case the weight of the $m$th element is $w_{TR}(\vec{s}_m) = N_r$ (if a uniform weighting of the retransmit/receive apertures was assumed).

## Coarray Reweighting

Two main aspects of the 2D aperture function determine the characteristics of an array. The geometry of the effective aperture, described by the SCA, and the weights that correspond to the subsequent elements, described by the coarray weighting function.

Based on eq. (5) it can be deduced that even using uniform weights for transmitting/receiving apertures can lead, in the case of redundant coarrays, to complex-shaped windows, possibly with sharp edges. These windows, like in classical signal processing problems, can result in high side-lobes levels, that can produce spurious image artifacts. Consequently, by changing the shape of the coarray weighting function it is possible to alter the side-lobes level and hence to influence the quality of the imaging algorithm. An arbitrary shape of the coarray weighting function can be obtained if apodization is applied for transmitting and receiving apertures.

Multiple physical apertures can have the same coarray. These arrays are called *coarray equivalent* and all of them have the same characteristics and the same imaging abilities.

In imaging applications involving synthetic focusing, the transmitters are excited subsequently and the received snapshots are subject to post-acquisition processing. Since apodization applied to the transmitting elements involves reduction of the emitted signal's amplitude, which in consequence reduces signal to noise ratio of the acquired data, here, we will assume that the weights will be applied only for the received signals in the post-acquisition step.

Redundancy in the coarray means that the number of transmission/reception cycles could be reduced, i.e., signals from some transmitter/receiver pairs could be omitted without the loss of resolution. On the other hand, however, averaging of multiple coarray observations improves signal to noise ratio. Therefore, if $m$th coarray element corresponds to $N_r$ transmitter/receiver pairs, and when the weights of the transmitters are $w(\vec{s}_{in}) = 1$, then the weights of the corresponding sensors are $w(\vec{s}_{jn}) = w(\vec{s}_m)/N_r$, where $w(\vec{s}_m)$ is the desired weight of the $m$th coarray element, for all $\vec{s}_{in}$ and $\vec{s}_{jn}$ satisfying $\vec{s}_m = \vec{s}_{in} + \vec{s}_{jn}$.

## Uniform Linear Array

To illustrate the coarray synthesis an example of a linear array consisting of 6 elements, presented in fig. 1a, will be used. VI independent excitations were performed to collect full matrix of data. The active elements used in the subsequent firings were indicated in fig. 1a, moreover the coarrays obtained for the successive firings are presented. When there is only one transmitting element, then according to eq. (2), the resulting aperture is the receiving aperture, shifted with the coordinates of the transmitter. Note that in some locations virtual elements occur repentantly in multiple excitation cycles. The number of repeated coarray elements is plotted versus their location in fig. 1b. From the figure it can be seen that there exists redundancy in the collected data, for instance, the virtual element at $x = 0$ occurred 6 times. This plot can also be interpreted as the effective aperture of the considered array. From fig. 1b it can

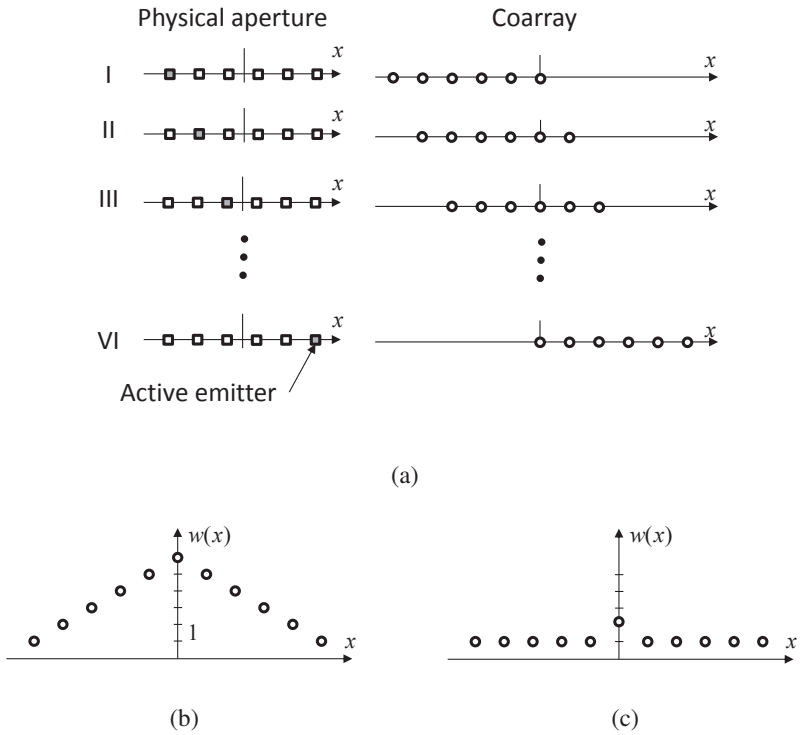


**FIGURE 1.** Linear array with indicated elements excited in the subsequent firings and the corresponding coarrays (a). Coarrays obtained as a result of $N_f = 6$ firings (I + II+...+VI) (b) and only $N_f = 2$ firings (I+VI) (c).

be seen that the effective aperture has much greater spatial extend compared to the physical array. Moreover, it can be seen that the resulting apodization has a triangle window shape.

The redundancy in the collected data can improve signal to noise ratio, however, it will not enhance angular resolution of the imaging system that is related to the array's spatial extent. From fig. 1a it can be seen that the outermost coarray elements emerge when the extreme elements from the physical array are excited. The coarray resulting as a sum of $N_f = 2$ firings, using external emitters, is presented in fig. 1c. The size of the aperture obtained from two firings is the same as that presented in fig. 1b. Moreover, it can be observed that only one element at $x = 0$ is redundant.

As it was explained in the previous section, by changing the weights of the receivers it is possible to obtain a desired shape of weighting function. An example of re-weighting procedure with the aim of obtaining a triangle-shaped weighting function is presented in fig. 2. Height of the bars, presented in the figure is proportional to the

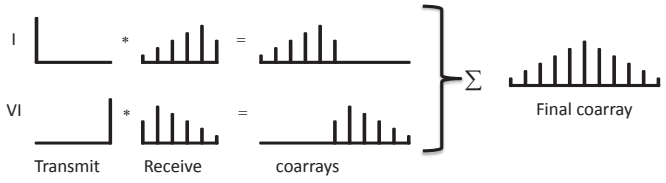


**FIGURE 2.** Example of the sparse array re-weighting with the aim of obtainining a coarray apodized with triangle weighting function.

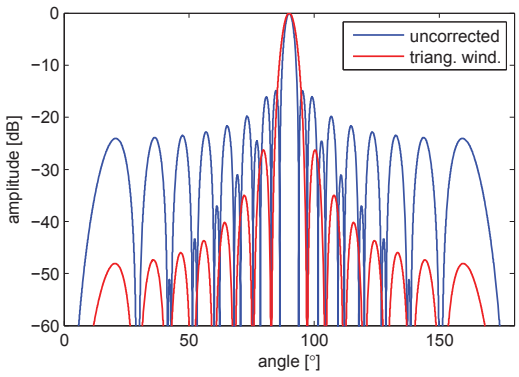


**FIGURE 3.** beampatterns of the triangle-shaped and uncorrected coarray obtained according to the scheme presented in fig. 1.

weights of the corresponding elements. In the considered case the weights of the sensors leading to redundancy were adjusted by a factor of 2 to avoid peaks in the final coarray.

To illustrate performance of the apertures obtained using the coarray approach, beampatterns of the coarrays of a triangle-shaped weighting function and a uniform coarray are presented in fig. 3. These coarrays were obtained in the way presented in figs. 1b and c respectively, however, the physical linear array consisted in this case of 16 elements, which lead to 31 coarray elements. From the figure it can be seen that the BP of the uniform coarray (obtained by firing two side elements) has the side-lobe level of -15dB, while for the triangle-window apodized coarray (obtained by firing all elements) this level is -27dB. However, the later BP exhibits wider main lobe than the previous one. Note that since the final coarrays presented in fig. 1b and 2 have the same shape, they have also the same BPs that can only differ by a constant gain and their plots will be identical after normalization.

The re-weighting procedure presented here can be changed to lead to different shapes of the weighting function, for instance Hamming window, as discussed in details in [6].

## STAR-LIKE COARRAY SYNTHESIS

In this section the principles of the coarray synthesis will be illustrated using an example of a 2D array. First, the physical aperture and its coarray will be presented, followed by the discussion concerning its performance. The influence of the redundancy of the obtained array and the respective beampatterns will be presented and the role of the coarray's re-weighting in the synthesis process will be discussed.

Various tools for analysis of imaging capabilities of the coarray will be used. In the first step, the response of the array will be evaluated using analytical approach assuming continues wave, i.e. steered response and beampattern. These tools provide a large number of information on the directionality characteristics based on the geometrical features of the aperture, however, cannot take into account the tone-burst excitation. Therefore, the imaging ability of the 2D apertures will be discussed farther using simulated data. A simplified simulation technique, based on the structure transfer function (STF) [11] will be used here. The approach allows to take into account arbitrary shape of the excitation signal as well as the dispersive nature of the structure.

The numerical simulations will be validated experimentally using a laser scanning vibrometer to sense PZT-excited waves in an aluminum plate.

### Star-shaped Aperture and Its Coarray

Advantages of coarray framework will be illustrated by an example of 2D sparse star-like array presented in fig. 4a. The array's inter-element spacing is $d = 5mm$. In the presented example the array will be steered to an angle of 90°, and the wavenumber will be adjusted to fulfill the condition $d = \lambda_0/2$.

As it was shown in the previous section, using the outermost elements of the array allows for obtaining the biggest spatial extent of coarray. Therefore, only these elements were used as transmitters, whereas the remaining elements

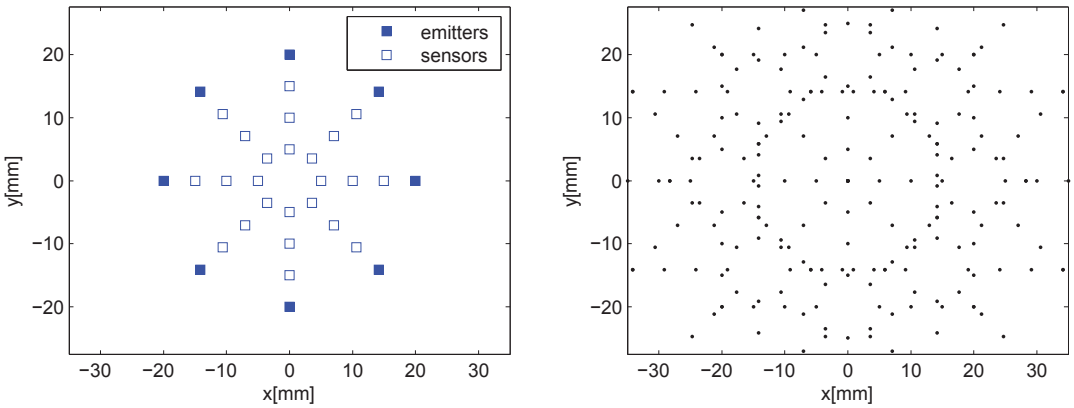


**FIGURE 4.** Star-like array with outer elements used as emitters (a) resulting sum coarray (b).

were used as sensors. No transmit/receive (pulse-echo) elements were used in the same measurement cycles.

The SCA of the star-shaped sparse aperture, presented in fig. 4b has rather complicated shape and, as expected, it has a bigger size compared to the physical array. In fig. 5a weighting function, which was obtained assuming uniform weighting of transmit and receive apertures was presented. The plot exhibits also the redundancy of the corresponding virtual channels. For instance, the weight of the central coarray element is 8, which means that 8 sums of vectors of transmitter/receiver pairs is equal to (0,0). Furthermore, there exists a few more elements with the redundancy of 2.

In figs. 6a, b and c steered responses of the considered coarray with different weighting functions are presented. In the first case, fig. 6a, apodization resulting form the data redundancy, (as shown in fig. 5a) was used. Next, uniform, rectangular-window was applied to the coarray to obtain fig. 6b. Finally, the coaray was re-weighted to obtain 2D Hamming-window, presented in fig. 5b and the resulting steered array pattern can be seen in fig. 6c.

All of these steered responses exhibit multiple side-lobes, additionally, multiple axes of symmetry can be seen in these characteristics, therefore, it is expected that it is sufficient to investigate the array's performance only for a small number of angles and the reaming direction will repeat these results.

To look closer at the side-lobes levels BPs obtained with different weighting functions were added in fig. 6d. Comparison of these characteristics shows that the uncorrected weighting function results in highest side-lobes level. Using the rectangular weighting function results in a slight reduction of side-lobes without any noticeable change of

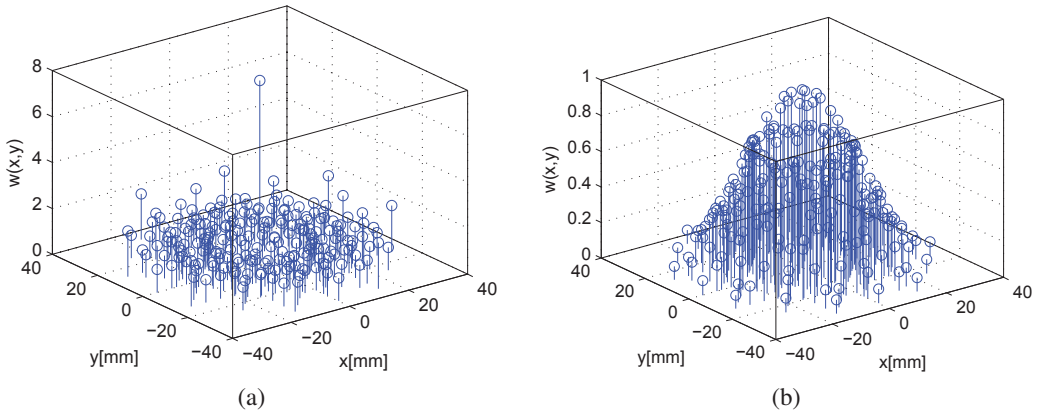


**FIGURE 5.** Weighting functions of coarray presented in fig. 4b. Uncorrected, resulting from the data redundancy (a), corrected by re-weighting with Hamming window (b).

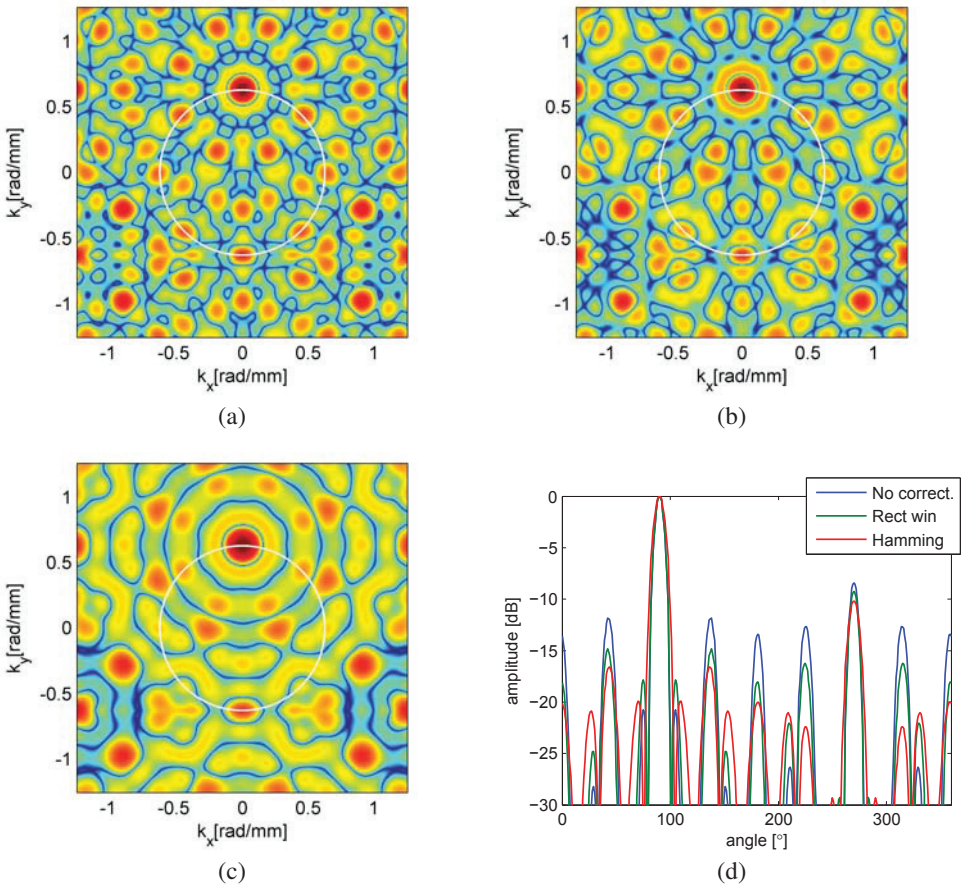


**FIGURE 6.** Steered responses of the star-like coarray with weighting: resulting from data redundancy, as presented in fig. 5a (a), rectangular window (b), Hanning window as shown in fig. 5b (c). Beampatterns obtained at points corresponding to white cycles presented in the figures (d).

the main-lobe width. As it could be expected, using Hamming window yields side-lobes reduction, however, the width of the main-lobe is also increased.

## Numerical Simulations

The simulations presented in this section were performed using STF approach, described in detail in [11]. The simulations were performed for a 2 mm aluminum plate. Tone burst-excitation signals consisting of 3 cycles of sine, at $150kHz$, modulated with Hanning window were used.

The first simulation result, presented in fig. 7a was obtained using uncorrected weighting, resulting from the data redundancy, i.e. with weighting function presented in fig. 5a. The image was analyzed to find maximal amplitudes that occurred for the subsequent angles. In fig. 7b this result can be compared to the BP obtained for the resulting coarray using the classical approach (point sources and no dispersion). An excellent agreement of the main lobes can be seen in the plot. However, the side-lobes are lower in the characteristics obtained from the STF image, thanks to the frequency-wavenumber information carried by the tone-burst signals.

In the next step, re-weighting was applied to obtain a uniform rectangular window and 2D Hamming window of the shape shown in fig. 5a. The resulting images are presented in figs. 8a and b respectively. Comparison of these images to that presented in fig. 7a shows that the highest insensitivity of the damage-related region exhibits the uncorrected

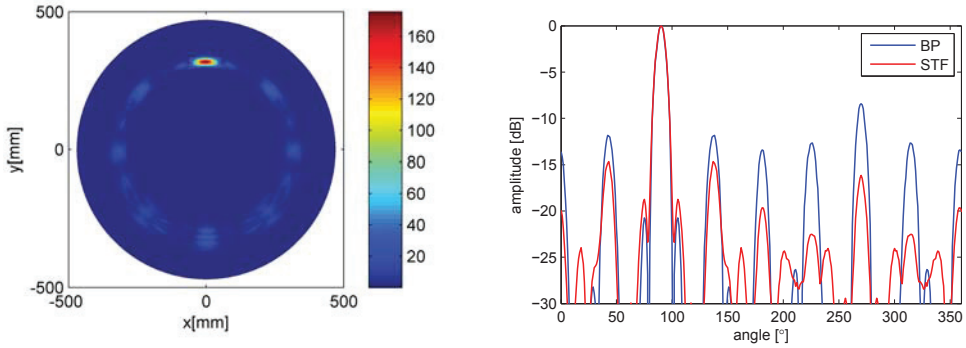


(a) (b)

**FIGURE 7.** Image of the far-field reflector obtained using the star-like coarray with weighting resulting from data redundancy presented in fig. 5a (a). Beampattern of the star-shaped coarray resulting form the array pattern and from post processing of structure transfer function image. (b)

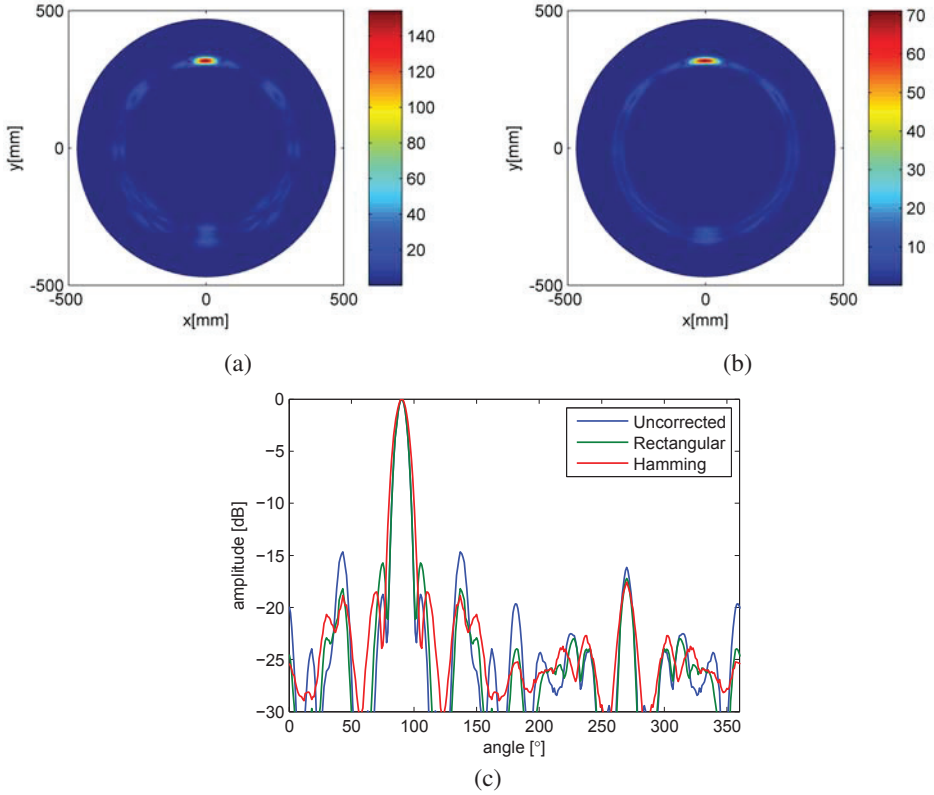


(a) (b)

(c)

**FIGURE 8.** Images of the far-field reflector obtained using the star-like coarray with uniform rectangular window (a), and Hanning window shown in fig. 5b (b). Directionality characteristics obtained by taking the maximal angular amplitudes of the upper images and the uncorrected image (c).

image. In other cases apodization is yields reduction of signals' weights, therefore, the resulting maximal intensity of the image is also reduced.

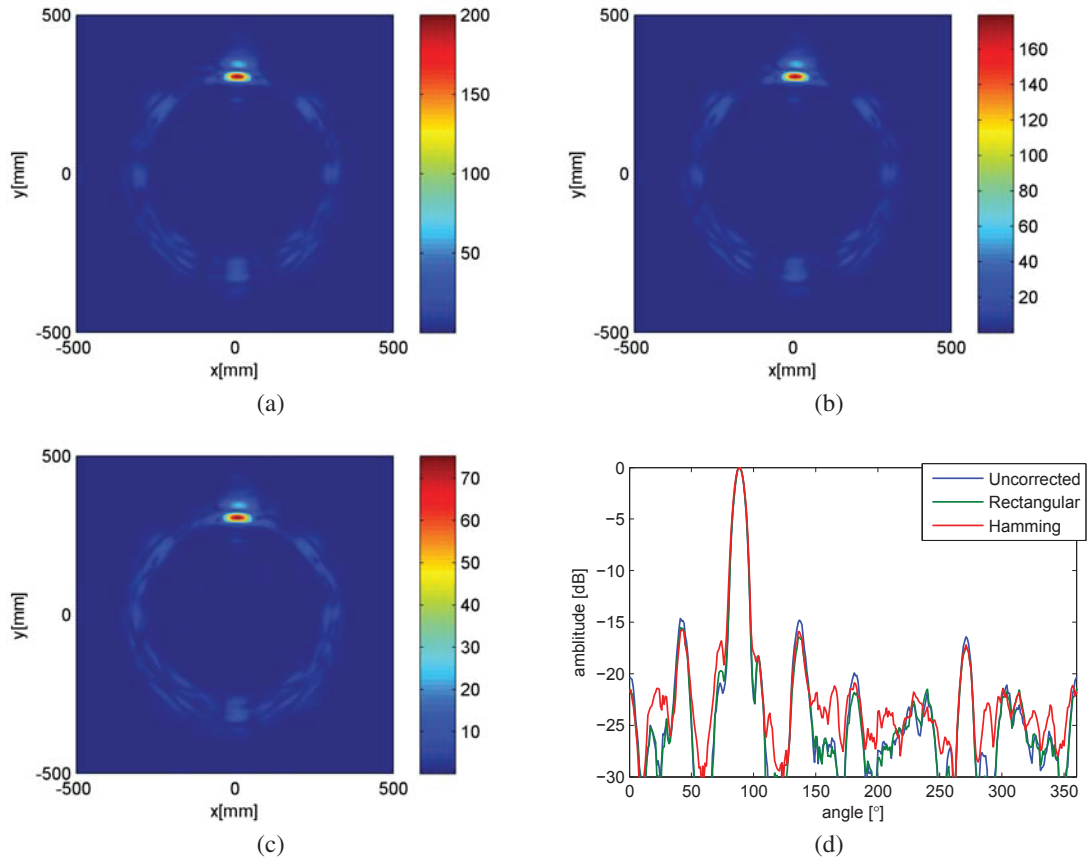


**FIGURE 9.** Images of the far-field reflector obtained using the star-like coarray with weighting resulting from data redundancy, as presented in fig. 5a (a), rectangular window (b), Hanning window as shown in fig. 5b (c). Directionality characteristics obtained by taking image amplitude at the points corresponding to white cycles presented in the figures (d).

In the next step, the images were analyzed to find maxima that occurred at subsequent angles. The results were normalized, which yielded directionality characteristics presented in fig. 8d. From these plots it can be seen that the uncorrected aperture leads to highest side-lobes among the investigated weighting functions. Moreover, it can be seen that application of Hamming window broadens the main-lobe and allows for obtaining the lowest side-lobes level among the considered cases; the differences, however, are not to significant.

## Experimental Results

The experiments presented below were performed to verify the simulations described in the previous sections. The investigated array topologies were using discrete PZT elements located at a 2mm thick Al plate and virtual receivers realized using scanning laser Doppler vibrometer. The virtual receiving apertures were created assuming inter-element distance of $d = \lambda_{A_0}/2 = 5mm$. Transmitting elements were excited by tone burst signals consisting of 3 cycles of sine, at $150kHz$, modulated with Hanning window were used for element. A small mass at a distance of $300mm$ and angle of $90^\circ$ with respect to the array was used as scatterer. Dispersion compensation was performed in all considered examples.

The aim of the experiment was to investigate the star-shaped setup presented in fig. 4a in a single transmitter multiple receivers (STMR) mode, in which the star-shaped grid of laser sensing points was used as a receiving aperture. The experiment consisted of eight steps, in which a single transmitter was moved for the emission to one of the locations of

the subsequent outermost array elements. The responses at the remaining 31 element positions were measured using vibrometer and the transmitter was moved to the next position and the next set of 31 signals was captured for that position.

Similarly to the simulations presented above, three apodization cases were investigated, i.e. the uncorrected weighting with inherent redundancy, the uniform rectangular weighting, and the reweighing using Hamming window. The results are presented in the the form of images that can be seen in figs. 9a, b and c, respectively. Significant differences of maximal insensitivity values that occurred in the images due to the re-weighting can be observed from the comparison of the image scales. To enable comparison of the directionality characteristics the normalized image amplitudes on the circles corresponding to the maximal echo amplitude are plotted in fig. 9c, which shows only minor differences between the cases.

## CONCLUSIONS

It was shown in the paper that the sum-coarray function, introduced by Hoctor and Kassam [8], facilitates the optimization process and enables avoiding redundancy in the topology of 2D arrays used in Lamb wave based imaging. Coarray is also an extremely useful tool when forming the resulting beampattern of a multistatic imaging setup due to the fact that it simplifies optimization of the element weighting function.

To introduce the coarray concept in the field of SHM, we first considered a linear uniform array, and than we presented the way how it can be used for analysis of the 2D array using a star-shaped transmitting/receiving sparse array. The SCA used in our simulations and experiments consisted of 32 elements. 8 outermost elements were used as transmitters that were fired sequentially in a single transmitter multiply receivers (STMR) mode. The resulting coarray consisted of 248 sensing elements and had rather complex shape.

We also illustrated how the coarray concept can be used for a straightforward beampattern optimization using apodization in the form of soft windows.

## ACKNOWLEDGMENTS

The presented work was financed within the research grant no. 2011/01/B/ST8/07210 “Theoretical basis for structural health monitoring by means of inverse problem solution under uncertainty” financed by the National Science Center of Poland.

## REFERENCES

1. H. Stankwitz, and S. Taylor, “Advances in non-linear apodization for irregularly shaped and sparse two dimensional apertures,” in *Radar Conference, 2005 IEEE International*, 2005, pp. 635–640.
2. M. Karaman, I. O. Wygant, O. Oralkan, and B. T. Khuri-Yakub, *IEEE Trans, on Medical Imaging* **28** (2009).
3. B. W. Drinkwater, and P. D. Wilcox, *NDT&E International* **39**, 525 – 541 (2006), ISSN 0963-8695.
4. L. Ambrozinski, *Advanced Structural Damage Detection: From Theory to Engineering Applications*, Wiley, 2013, chap. Beamforming of guided waves, pp. 177–210.
5. J. Davies, F. Simonetti, M. Lowe, and P. Cawley, *AIP Conference Proceedings* **820**, 142–149 (2006).
6. L. Moreau, B. Drinkwater, and P. Wilcox, *IEEE Trans. on UFFC* **56**, 1932 –1944 (2009).
7. G. R. Lockwood, P.-C. Li, M. O’Donnell, and F. S. Foster, *IEEE Trans. on UFFC* **45** (1998).
8. R. Hoctor, and S. Kassam, *Proceedings of the IEEE* **78**, 735–752 (1990), ISSN 0018-9219.
9. L. Ambrozinski, T. Stepinski, and T. Uhl, “2D aperture synthesis for development of Lamb wave imaging using co-arrays,” in *Proc. SPIE 9064*, 2014.
10. G. R. Lockwood, P.-C. Li, M. OŠDonnell, and F. S. Foster, *IEEE Transactions On UFFC* **43** (1996).
11. L. Ambrozinski, T. Stepinski, and T. Uhl, *Journal of Intelligent Material Systems and Structures* (2014 (accepted)).